
# Raman spectroscopy of supersonic jets of CO 2 : Density, condensation, and translational, rotational, and vibrational temperatures

B. Maté, G. Tejeda, and S. Montero

Citation: The Journal of Chemical Physics **108**, 2676 (1998); doi: 10.1063/1.475660

View online: http://dx.doi.org/10.1063/1.475660

View Table of Contents: http://scitation.aip.org/content/aip/journal/jcp/108/7?ver=pdfcov

Published by the AIP Publishing



# Raman spectroscopy of supersonic jets of $CO_2$: Density, condensation, and translational, rotational, and vibrational temperatures

B. Maté, G. Tejeda, and S. Montero
*Instituto de Estructura de la Materia, CSIC, Serrano 121, 28006, Madrid, Spain*

(Received 30 January 1997; accepted 11 November 1997)

The links between translational, rotational, and vibrational temperatures of supersonic molecular jets, and their density and degree of condensation, are discussed in terms of quantitative Raman scattering experimental data. Such links are established as the result of energy and momentum conservation laws, and of the collisional regime in the jet. Four representative supersonic expansions of $CO_2$, generated at different stagnation pressures are analyzed, showing the potential of quantitative Raman spectroscopy for a complete characterization of the jet. © *1998 American Institute of Physics.* [S0021-9606(98)00907-6]

## I. INTRODUCTION

Local density number ($\mathcal{N}$), temperature ($T$), and flow velocity ($\overline{v}$), are the quantities most commonly used to characterize macroscopically the flow field of a supersonic jet at any point $(x,y,z)$. In addition, in a wide domain of pressures and temperatures, real gases tend to partially condense. This process is not neutral energetically and must be considered jointly with the aforementioned quantities.

In the widely used approximation known as the isentropic model for the expansion of a perfect gas,[1,2] the condensation is ignored and the temperature is regarded as single quantity. However, it is well established that molecular supersonic jets are systems far out from thermodynamical equilibrium which, to a greater or lesser extension, do not obey globally the Maxwell–Boltzmann distribution law. Therefore, in the molecular jet the concept of temperature cannot be defined unambiguously by a single quantity. Nonetheless, as the energies of the molecular quantum levels associated with translational, rotational, or vibrational degrees of freedom may differ in orders of magnitude, local Maxwell–Boltzmann distributions are usually found for the three kinds of motions. It is hence meaningful to talk about translational ($T_t$), rotational ($T_r$), and vibrational ($T_v$) temperatures, as they account for the mean width of the local distributions of energy.[3–5] Still, as the jet is highly anisotropic in space, it may be necessary to distinguish between parallel ($T_\parallel$) and perpendicular ($T_\perp$) translational temperatures, which account for the spread of molecular translational velocities parallel and perpendicular to the flow field lines, respectively. Such a distinction between $T_\parallel$ and $T_\perp$ appears to be necessary just beyond the quitting surface,[6] where the collisional regime is very faint. Otherwise, $T_\parallel$ and $T_\perp$ may be considered in equilibrium.[7]

An accurate knowledge of the spatial distribution of translational, rotational, and vibrational temperatures in the jet is essential for the comprehension and quantification of the complex relaxation processes governing the interchange of energy.[8] The physical principles, practical difficulties, and limitations for the determination of translational, rotational, and vibrational temperatures under supersonic flow regime have been discussed in connection with the electron impact induced fluorescence (EIF) technique.[3,9–11] Examples of translational and rotational temperature data from EIF experiments can be found in the literature for a number of specific problems[4,5,7,12] but, for systems where the vibrational degrees of freedom are populated at the temperature of the experiment, data are sparse. On the other hand, establishing the condensation degree of the jet with some accuracy is a difficult problem, particularly in the region not too far downstream from the nozzle.

Laser-induced fluorescence (LIF),[13,14] linear Raman spectroscopy,[11,15–18] nonlinear Raman spectroscopy,[19–23] and third-harmonic nonlinear generation,[24,25] have proved efficient for the attainment of rotational and vibrational temperatures in a wide spatial domain of the jet. Rayleigh scattering, combined with linear Raman spectroscopy, has provided a measure of the density number in the jet.[26] In turn, local translational temperatures have been so far more elusive to these experimental methods.[27] These techniques, though apparently less demanding from the experimental point of view than EIF, have been oriented largely toward spectroscopic, rather than to gas dynamics problems. In addition to spectroscopy-based experiments, time-of-flight techniques allow measuring parallel translational temperatures ($T_{\parallel,\infty}$) in the region of the jet far downstream in the expansion.[28–30] The combination of stimulated Raman spectroscopy (SRS) with time-of-flight data has proved to be a powerful approach for the study of rotational relaxation.[31]

Supersonic expansions of $CO_2$ have been the subject of a number of experimental works considering different aspects of the problem on the basis of various techniques. A mapping of condensation in $CO_2$ jet plumes has been carried out by means of Rayleigh scattering.[32] Jet density and temperature were measured by means of electron beam absorption and luminescence methods.[33] The effect of source pressure, source temperature, and dimension and form of nozzle onto the size of clusters[34] as well as the kinetics of cluster formation, particularly of dimers and trimers,[35–37] has been investigated by means of mass spectrometry. Relaxation rates and lag between vibrational, rotational, and translational temper-

 

atures,[29,38] and center line intensities of the jet[6] have been studied by means of time-of-flight experiments. Conclusions about the effect of temperature and pressure onto condensation and vibrational relaxation,[39] and the role of molecular internal degrees of freedom in the energy transfer[40] were based on electron impact fluorescence experiments; IR radiation from the jet provided information about local density in order to establish further links between condensation and vibrational relaxation.[41] The deviations of rotational temperature in the jet from the isentropic prediction have been measured by means of intracavity Raman spectroscopy;[16,17] Rayleigh scattering has proved useful to track the onset of condensation in some detail.[17]

As far as the detailed structure of the condensed fraction of the jet is concerned, high resolution IR spectroscopy has been successful in establishing the geometry of the $CO_2$ dimers[42,43] and trimers[44,45] formed in the jet. Large clusters have been investigated by Fourier transform infrared spectroscopy (FTIR).[16] In turn, coherent anti-Stokes Raman spectroscopy (CARS) has provided insight about vibrational properties[47–51] and formation kinetics of small clusters.[52,53]

The works mentioned above have revealed many partial aspects of the supersonic expansions of $CO_2$. To some extent, the present work aims to provide a global vision of the problem. This is attempted on the sole basis of experimental data from a single Raman scattering experiment. We propose here the following procedure to derive the remaining relevant quantities of a molecular jet: Combining the experimental data of density number ($\mathcal{N}$), rotational temperature ($T_r$), and vibrational ($T_v$) temperature in a system of three equations of conservation of linear momentum, conservation of energy, and rotational-translational relaxation, the three remaining unknown functions of translational temperature ($T_t$), condensation energy ($\chi$), and flow velocity ($v$), are deduced.

In principle, $\mathcal{N}$, $T_r$, and $T_v$ can be provided by some other spectroscopic technique, or combination of them, but only linear Raman spectroscopy appears to able to provide enough spatial resolution (see below), and accuracy in the determination of $\mathcal{N}$ in a range of, at least, five orders of magnitude while $T_r$ and $T_v$ are simultaneously measured in the same experiment.

We substantiate the proposed procedure with the experimental Raman data from four supersonic continuous jets of pure $CO_2$, henceforth referred to as expansions I, II, III, and IV, generated at room temperature with stagnation pressures $P_0^{\mathrm{I}} \simeq 203$ kPa, $P_0^{\mathrm{II}} \simeq P_0^{\mathrm{I}}/2$, $P_0^{\mathrm{III}} \simeq P_0^{\mathrm{I}}/5$, and $P_0^{\mathrm{IV}} \simeq P_0^{\mathrm{I}}/9$ through a circular nozzle of diameter $D = 300\ \mu$m. The analogies and differences among these jets is discussed here in terms of the relations between density, translational, rotational, vibrational temperatures, and condensation degree, and are compared with the results from previous works on supersonic jets of $CO_2$.

## II. THEORY

The method outlined here is for the axial points $(0,0,z)$ of a steady axis-symmetric jet expanding along $z$, consisting of a single molecular species. In the present version it applies to the zone of silence of the jet between the nozzle (sonic surface) and either the quitting surface, or the first normal shock front, whichever is first. In this region the rate of collisions may be considered high enough to maintain the equilibrium $T_\parallel = T_\perp = T_t$ between the parallel and perpendicular components of the translational temperature.[7] On the contrary, the relation between rotational and translational temperatures range from nearly equilibrium betweem them, to nonequilibrium, depending markedly on the stagnation conditions of pressure and temperature, and on the points of the zone of silence considered. Finally, vibrational temperature is out of equilibrium with the rotational and translational temperatures from the very beginning of the expansion.

The summational invariance of momentum along $z$ may be expressed at the point $(0,0,z)$ of the jet symmetry axis as[1,2,54]

$$v\,\frac{\partial v}{\partial z} + \frac{1}{\mathcal{N} W}\,\frac{\partial P}{\partial z} = 0, \tag{1}$$

where $v$ (in m/s), $\mathcal{N}$ (in mol/m$^3$), and $P$ (in Pa) are, respectively, the flow velocity, the molar density number, and the pressure at the point $(0,0,z)$, referred to an origin located at the nozzle; $W$ (in kg/mol) is the molar mass of the expanded gas. The conservation of total energy can be expressed in terms of the molar enthalpy $H$ (in J/mol) in the form

$$v\,\frac{\partial v}{\partial z} + \frac{1}{W}\,\frac{\partial H}{\partial z} = 0. \tag{2}$$

As an additive quantity,[55,56] the jet enthalpy can be expressed to a good approximation in terms of the translational, rotational, and vibrational enthalpies, and of the condensation enthalpy, by means of the corresponding temperatures, $T_t$, $T_r$, $T_v$, and of the condensation energy, $\chi$, in the form

$$H = H_t(T_t) + H_r(T_r) + H_v(T_v) + \chi, \tag{3}$$

where $T_t$, $T_r$, and $T_v$ are defined by local Maxwell-Boltzmann distributions of population; the condensation energy $\chi = \alpha E$ is the product of the condensed molar fraction, $\alpha$, times the molar condensation energy, $E$.

From the definition of molar heat capacity at constant pressure, $C_P = \partial H/\partial T$, the gradient of the enthalpy along the expansion axis may be expressed in terms of the translational, rotational, and vibrational contributions to the heat capacity, $C_{P,t}$, $C_{P,r}$, and $C_{P,v}$, respectively, and of the thermal and condensation energy gradients along $z$, in the form

$$\frac{\partial H}{\partial z} = C_{P,t}\,\frac{\partial T_t}{\partial z} + C_{P,r}\,\frac{\partial T_r}{\partial z} + C_{P,v}\,\frac{\partial T_v}{\partial z} + \frac{\partial \chi}{\partial z}. \tag{4}$$

Substituting Eq. (4) into Eq. (2), combining Eq. (2) with Eq. (1), and expressing the pressure in terms of the translational termperature as $P = \mathcal{N} R T_t$, the resulting differential equation

$$(C_{P,t} - R)\,\frac{\partial T_t}{\partial z} + C_{P,r}\,\frac{\partial T_r}{\partial z} + C_{P,v}\,\frac{\partial T_v}{\partial z} + \frac{\partial \chi}{\partial z} - \frac{R}{\mathcal{N}}\,\frac{\partial \mathcal{N}}{\partial z}\,T_t = 0, \tag{5}$$

relates the thermal and density number gradients along $z$ with the translational temperature and condensation energy. Under the equilibrium condition $T_{\parallel}=T_{\perp}=T_t$, the translational contribution to the molar heat capacity at constant pressure is $C_{P,t}=5R/2$ for all atoms and molecules; $R=8.3145\ \mathrm{J\,K^{-1}\,mol^{-1}}$ is the molar gas constant. This allows rewritting Eq. (5) in the more convenient form

$$\frac{\partial T_t}{\partial z}+p(z)T_t=q(z), \tag{6}$$

where

$$p(z)=-\frac{2}{3\mathscr{N}}\frac{\partial \mathscr{N}}{\partial z}, \tag{7}$$

and

$$q(z)=-\frac{2}{3R}\left(C_{P,r}\frac{\partial T_r}{\partial z}+C_{P,v}\frac{\partial T_v}{\partial z}+\frac{\partial \chi}{\partial z}\right). \tag{8}$$

For $T_r$ above the characteristic rotational temperature, $\Theta_r$, a good approximation for the rotational heath capacity is $C_{P,r}=N_rR/2$, where $N_r=2$ (linear) or $N_r=3$ (nonlinear) is the number of rotational degrees of freedom.[55–57] For $T_r$ below $\Theta_r$, $C_{P,r}$ must be derived from the rotational partition function at the rotational temperature.[55] For $T_v<300$ K the vibrational contribution to the heat capacity of a polyatomic molecule of $n$ atoms is described to a good accuracy by[55]

$$C_{P,v}=R\sum_{i=1}^{N_v}\frac{(x\omega_i)^2e^{-x\omega_i}}{(1-e^{-x\omega_i})^2}, \tag{9}$$

with $N_v=3n-5$ (linear) or $N_v=3n-6$ (nonlinear) being the number of vibrational degrees of freedom; $\omega_i$ are the $N_v$ harmonic vibrational wave numbers, and $x=hc/kT_v=1.4388/T_v$ for $\omega_i$ in $\mathrm{cm^{-1}}$ and $T_v$ in kelvin.

For the domain of $z$ where $p(z)$ and $q(z)$ are continuous, the general solution of Eq. (6) is

$$T_t(z)=e^{-G(z)}\left(c+\int e^{G(z)}q(z)dz\right), \tag{10}$$

with

$$G(z)=\int p(z)dz=-\frac{2}{3}\ln\mathscr{N}+c', \tag{11}$$

where $c$ and $c'$ are constants to be fixed from the boundary conditions of the experiment. Here we choose imposing the critical temperature ($T^*$) and the critical molar density number ($\mathscr{N}^*$) at the onset of the supersonic regime,[1,2] with Mach number $M=1$ at $z=0$, the sonic plane of the nozzle.

By virtue of Eqs. (10) and (11), and of the boundary conditions, the translational temperature may be expressed as a function of the experimental quantities $\mathscr{N}$, $T_r$, $T_v$, and of the total condensation energy $\chi(z)=\alpha E$, so far an unknown function, in the form

$$T_t(z)=\left(\frac{\mathscr{N}}{\mathscr{N}^*}\right)^{2/3}\left[T^*+\int\left(\frac{\mathscr{N}}{\mathscr{N}^*}\right)^{-2/3}q(z)dz\right]. \tag{12}$$

In order to first determine from experiment the global condensation energy function $\chi(z)$ included in $q(z)$, an auxiliary equation is required. The rotational–translational relaxation equation,[29,58] rewritten as

$$T_t(z)=T_r(z)+v\left(\frac{dT_r}{dz}\right)\tau_r, \tag{13}$$

is useful for this purpose. The rotational–translational relaxation time is given by

$$\tau_r=Z_r\ \tau_{\mathrm{coll}}, \tag{14}$$

where $Z_r$ is the average number of collisions required to attain the equilibrium $T_r=T_t$ and

$$\tau_{\mathrm{coll}}=\left(4N_A\mathscr{N}\sigma^2\sqrt{\frac{\pi RT_t}{W}}\right)^{-1} \tag{15}$$

is the average time between collisions; $N_A$ is Avogadros's constant, and $\sigma$ an effective collision diameter ($\sigma=3.996$ Å for $CO_2$).[8] Equating the right-hand terms (RHT's) of Eqs. (12) and (13), and numerically solving the resulting equation, the global condensation energy function $\chi(z)$ may be obtained. Since neither the flow velocity $v$ nor the relaxation time $\tau_r$ in Eq. (13) is known *a priori*, an iterative procedure is required. Accordingly, in the initial iteration cycle, the flow velocity in Eq. (13) and the translational temperature in Eq. (15) are approximated by their isentropic values. In the subsequent iterations these quantities are replaced by the values from the preceding cycle, in order to improve the accuracy of the unknown variables in the jet, $\chi$ and $T_t$. However, the convergence is fast and the initial cycle already provides an approximate picture of the properties of the jet in the zone of silence.

After the first iteration, once the translational temperature and the condensation energy have been established, the flow velocity at the point $m$ is

$$v(m)=\sqrt{\frac{2(E_t+E_r+E_v-\chi)}{W}}, \tag{16}$$

as deduced from the integral form of Eq. (2). The terms

$$E_t=\frac{5R}{2}\left[T_0-T_t(m)\right], \tag{17}$$

$$E_r=\frac{N_rR}{2}\left[T_0-T_r(m)\right], \tag{18}$$

$$E_v=U_v(T_0)-U_v(T_v(m)), \tag{19}$$

account, respectively, for the partial conversion of translational, rotational, and vibrational energy of the stagnation reservoir at the temperature $T_0$ into kinetic energy of the directed flow, at the point $m$; $U_v$ is the internal vibrational energy, which depends just on the vibrational temperature and vibrational wave numbers. In the harmonic approximation it is given by[55]

$$U_v=RT_v\sum_{i=1}^{N_v}\frac{(x\omega_i)e^{-x\omega_i}}{(1-e^{-x\omega_i})}. \tag{20}$$

According to Eq. (16), it should be noticed that the flow velocity of a real gas is larger than that predicted by the

isentropic approximation of a perfect gas. In the real gas there is a vibrational contribution $E_v \geqslant 0$ and, in addition, the energy released by condensation is such that $\chi \leqslant 0$. Depending on the particular stagnation conditions of the jet and on the molecular species involved, these two contributions may be neglegible or, on the contrary, may represent a substantial increase of the flow velocity.

The Mach number at the point $m$, $M(m)=v(m)/a(m)$ can be obtained here from the experimental data, without the approximations implicit in the isentropic model for the expansion of a perfect gas; $v(m)$ is known from Eqs. (16) to (20), and the local velocity of sound at $m$ is given by

$$a(m)=\sqrt{\frac{RT_t(m)\gamma(m)}{W}}, \tag{21}$$

where $\gamma(m)=C_P/C_V$ is the local ratio of heat capacities at constant pressure and volume at the point $m$ of the expansion axis; $C_P=C_{P,t}+C_{P,r}+C_{P,v}$ is known from the experimental data since it depends just on the vibrational temperature at the point $m$, while $C_V=C_P-R$. Due to the different rate of increment of velocity and temperature, deviations from the parametric description of the Mach number[59,60] may be expected in the case of condensation.

As far as Eqs. (7), (8), (12), and (13) are concerned, the experimental data of density number $\mathcal{N}$ and the gradients of the temperatures $T_r$ and $T_v$, required to generate the function $q(z)$, are measured in the Raman scattering experiment at discrete points of $z$, rather than as analytical functions. Therefore, it is advantageous to replace Eqs. (12) and (13) by equivalent forms in terms of discrete points $m$ of the expansion symmetry axis, instead of the continuous variable $z$. The pertinent algorithm is described in the Appendix.

Finally, it should be mentioned that if the condensation energy is neglected in Eq. (12), the vibrational temperature frozen, and the density number replaced by its isentropioc description,[1,2] then Eq. (12) leads to the identity of translational and rotational temperatures proper for the isentropic approximation. According to Eq. (13) this implies an infinitely short rotation–translation relaxation time.

## III. EXPERIMENT

### A. Instrumentation

The very high sensitivity Raman spectrometer[61] used in the present work is equipped with a 2360 lines/mm holographic grating as dispersive element, and a 512×512 pixel charge-coupled device (CCD) detector refrigerated by liquid $N_2$. For an excitation power of 2 W at the 514.5 nm line of a cw-$Ar^+$ laser, the routine detection limit of the instrument, referred to vibrational bands of gas phase samples, is on the order of $4\times10^{-5}$ mol/m$^3$ at a spectral resolution of 1 cm$^{-1}$. This allows recording Raman spectra of a quality good enough to extract information about density number, rotational temperatures, and vibrational temperatures in the highly rarefied $CO_2$ continuous jets studied here.

The jets have been generated by expansion of the gas into a low pressure chamber through a miniature capillary nozzle of diameter $D=300$ $\mu$m and length $L\simeq1$ mm, satisfying the recommended efficiency condition[62] $L/D\geqslant2$. The core of the jets consists of a *zone of silence* which remains isolated from the environment by a well-defined system of barrel and normal shock waves. This *zone of silence* approaches the ideal conditions of a perfect vacuum.[62]

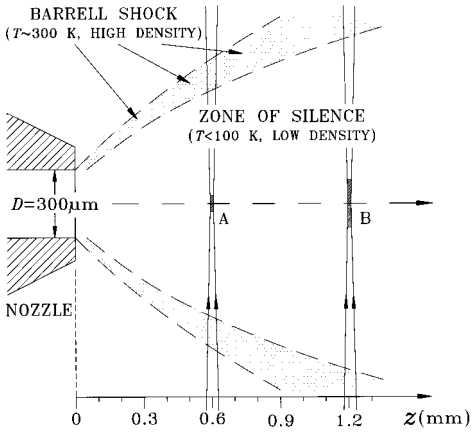


FIG. 1. Representative recording conditions of a Raman spectrum at $z=0.6$ mm (A) and at $z=1.2$ mm (B), drawn at scale, showing the actual spatial resolution. Dashed sections of the laser beam (A)—(14×70 $\mu$m), and (B)—(14×220 $\mu$m), are the scattering zones ''seen'' by the CCD detector.

The low pressure chamber of $42\times42\times30$ cm$^3$, manufactured in aluminum, is connected to a vacuum system consisting of a rotary pump of 70 m$^3$/h plus a Roots pump of 400 m$^3$/h. For the continuous jet of higher flow rate, generated at a nominal stagnation pressure $P_0^1=203$ kPa, this system is capable of maintaining the residual pressure below 0.4 hPa for hours. Three optical windows at the front, back, and bottom of the chamber allow using it as a large Raman gas cell operating at very low pressure. The nozzle, located inside of the chamber, is movable along three orthogonal directions in space by means of remote-controlled microactuators. It can be positioned along the expansion axis ($z$ axis) with a relative accuracy of $\pm1$ $\mu$m. The absolute accuracy of the distance $z$ between the nozzle and the focal spot of the exciting laser beam is about $\pm50$ $\mu$m (see Fig. 1).

The exciting laser beam is sharply focused with a lens of focal length $f=35$ mm, forming a beam waist of diameter about 14 $\mu$m. This figure represents the spatial resolution along $z$. The spatial resolution across $z$ can be controlled with the readout of the CCD detector by selecting the signal from just a narrow central track of pixels. In this way a spatial resolution of up to 70 $\mu$m can be attained across the jet, as shown in Fig. 1(A). Such a good resolution can only be attained near the nozzle, up to 1 mm away, where the intensity of the Raman signal is still high enough. For distances between 1 and 2 mm from the nozzle the Raman spectra have been recorded at a cross-spatial resolution of 220 $\mu$m [Fig. 1(B)], and for distances above 2 mm, the resolution was reduced to 1100 $\mu$m. Points near the borders between these three regions were recorded at both resolutions in order to guarantee the smooth concatenation of the data $\mathcal{N}$, $T_r$, and $T_v$ along $z$. With this procedure, the data $\mathcal{N}$, $T_r$, and $T_v$ are recorded from small enough spatial regions, which truly represent the local properties of the expansion axis. One must emphasize that such high spatial resolution is

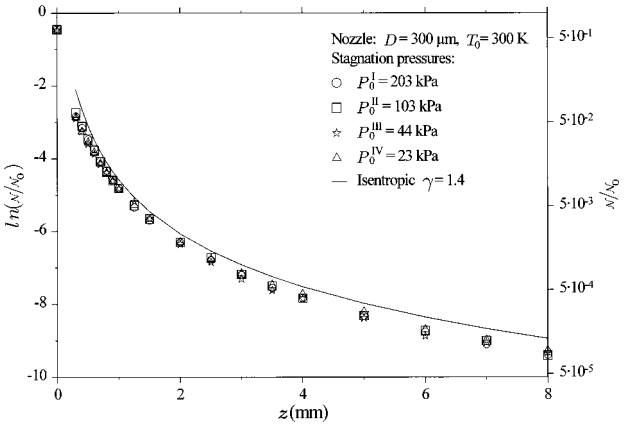


FIG. 2. Molar density number $\mathcal{N}$ in supersonic expansions I–IV of $CO_2$; $\mathcal{N}_0^{I}=81.24$, $\mathcal{N}_0^{II}=41.19$, $\mathcal{N}_0^{III}=17.55$, and $\mathcal{N}_0^{IV}=9.18$ mol/m$^3$.

a unique feature of linear Raman spectroscopy, which allows probing the region near the nozzle—to as close as 0.3 mm—without interference from the much denser and warmer region of the lateral barrel shock boundary.[18]

### B. Methodology

Due to the limited capacity of the vacuum system, the four expansions studied here show a normal shock front at about 10 mm downstream from the nozzle. Thus, only the region up to about $z=8$ mm can be regarded as a zone of silence free of perturbation. On the other hand, axial points at $z<0.3$ mm are hardly accessible with the present setup.

For the interval free from perturbation, $0.3\leqslant z\leqslant 8$ mm, the relative molar density number, $\mathcal{N}(m)/\mathcal{N}(m')$, between the points $m$ and $m'$ has been determined from the ratio of Raman intensities of the vibrational band ($Q$ branch) of $CO_2$ at 1388 cm$^{-1}$,

$$\frac{I_{1388}(m)}{I_{1388}(m')}=\frac{\mathcal{N}(m)}{\mathcal{N}(m')}\,\frac{Z[T_v(m')]}{Z[T_v(m)]}, \tag{22}$$

measured at $m$ and $m'$; $Z[T_v(m)]$ and $Z[T_v(m')]$ are the vibrational partition functions for the corresponding vibrational temperatures (see below).

Relative values can be converted into absolute molar density numbers, comparing the intensity measured at a given reference point of the jet with the intensity from a static sample of $CO_2$ at a reference pressure of 100 hPa without modifying the optical conditions of the experiment. In order to check the consistency, this procedure was repeated at three different points of the jet ($z=1$ mm, $z=2$ mm, and $z=3$ mm). A dispersion of about $\pm 6\%$ was found. Absolute molar density numbers $\mathcal{N}$ have been measured accurately just for expansion I. The corresponding absolute density numbers of expansions II, III, and IV have been normalized by means of the stagnation pressure. The absolute values of $\mathcal{N}$, required to estimate the average time between collisions, are shown in Fig. 2. Otherwise, just relative densities are required, as deduced from Eqs. (5), (7), and (12).

The rotational temperature $T_r(m)$ at a point $m$ has been measured from the relative Raman intensities, $I_J(m)$, of several $J\rightarrow J+2$ rotational transitions, given for $CO_2$ by

$$I_J(m)=C\mathcal{N}\,\frac{(J+1)(J+2)}{(2J+3)}\times\frac{\exp[-\beta BJ(J+1)/T_r(m)]}{\Sigma_J(2J+1)\exp[-\beta BJ(J+1)/T_r(m)]}, \tag{23}$$

with $C$ a constant, $J$ the rotational quantum number ($J$=even), $\beta=hc/k=1.4388$ K/cm$^{-1}$, and $B=0.390\,27$ cm$^{-1}$ the rotational constant of $CO_2$. In the region $0.3\leqslant z\leqslant 8$ mm no deviation from a Maxwell–Boltzmann distribution law has been observed.

The vibrational temperature, $T_v(m)$, at a point $m$ has been determined from the ratio of intensities

$$\frac{I_{1409}(m)}{I_{1388}(m)}=2\,\frac{\langle 667|\overline{\alpha}|2076\rangle^2}{\langle 0|\overline{\alpha}|1388\rangle^2}\,\exp[-\beta 667/T_v(m)], \tag{24}$$

of the $Q$ branches of the $667\rightarrow 2076$ cm$^{-1}$ double degenerate vibrational transition, observed as a hotband at 1409 cm$^{-1}$, and of the $0\rightarrow 1388$ cm$^{-1}$ transition from the ground state, observed at 1388 cm$^{-1}$. The vibrational transition moments of the polarizability are:[63] $\langle 0|\overline{\alpha}|1388\rangle=6.79\times 10^{-42}$ C V$^{-1}$ m$^2$, and $\langle 667|\overline{\alpha}|2076\rangle=7.20\times 10^{-42}$ C V$^{-1}$ m$^2$.

Because of stray light from the nozzle tip, the Raman spectra recorded at distances within 0.3 mm from the nozzle are too noisy. The quality of the corresponding density and temperature data are certainly not better than the estimates made by nonlinear interpolation between the data corresponding to the imposed boundary condition $M=1$ at $z=0$, the so-called critical density number $\mathcal{N}^*$ and critical temperature $T^*$, and the experimental data for the first few probing points at $z\geqslant 0.3$ mm. A function of the form

$$\ln y=a_0+a_1z+a_2z^2, \tag{25}$$

has been used for the interpolation; $y$ stands for the density number, or for the rotational temperature.

The experimental quantities $\mathcal{N}$, $T_r$, and $T_v$ are subject to two sources of uncertainty, with accumulative effects. The first one is the measurement process of Raman intensities according to Eqs. (22)–(24). The second, since $\mathcal{N}$, $T_r$, and $T_v$ depend on $z$, the uncertainty of up to $\pm 50$ $\mu$m in the absolute position $z$. The latter source of uncertainty is particularly important in the region near the nozzle, up to about 1 mm away, where the density and thermal gradients are very large. Since Raman intensities decay dramatically with the distance from the nozzle, it is difficult to establish a figure of confidence for each measured quantity and point of the jet. An estimate from comparing different series of experiments (see Figs. 2–4) suggests that the relative values of $\mathcal{N}$ are accurate to 10% along the whole interval studied here, and $T_r$ accurate to $\pm 5$ K for $z<1$ mm, or to $\pm 3$ K for $z>1$ mm. The accuracy of $T_v$ is lower because of the inherent low cross section of the hotband at 1409 cm$^{-1}$ used for that purpose, probably not better than $\pm 5$ K for expansions I and II, and $\pm 10$ K for expansions III and IV.

The above uncertainties add up when the experimental data are introduced into Eqs. (12) and (13). An additional source of uncertainty must still be considered: The integral in Eq. (12) is replaced by the discrete summation between the limits $z=0$ and $z=z_m$, as described in the Appendix. This

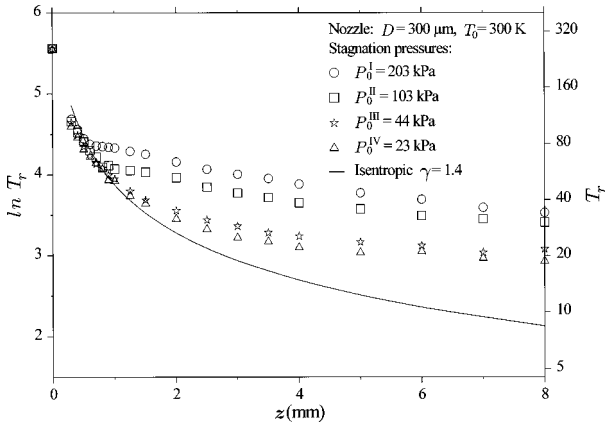


FIG. 3. Rotational temperatures in supersonic expansions I–IV of $CO_2$.

summation is affected by the difficulty of obtaining reliable experimental data very close to the nozzle. These data have been replaced here by the nonlinear interpolation of $\mathcal{N}$ and $T_r$ described by Eq. (25), for $0 \leqslant z < 0.3$ mm, at steps of 0.05 mm. Because of the strong thermal and density gradients for $0 \leqslant z < 0.3$ mm, such a fine discretization step is required in order to minimize numerical errors. For a step of 0.05 mm, the influence of accumulative numerical errors onto the accuracy of the translational temperature at points $z \geqslant 0.3$ mm is neglegible compared to the uncertainties of the experimental data $\mathcal{N}$, $T_r$, and $T_v$.

## IV. RESULTS AND DISCUSSION

The four continuous $CO_2$ jets, I–IV, investigated along the $z$ axis in the range of distances $0.3 \leqslant z \leqslant 8$ mm from the nozzle, have been generated at nominal stagnation pressures $P_0^{I}=203$, $P_0^{II}=103$, $P_0^{III}=44$, and $P_0^{IV}=23$ kPa. The complete set of raw data $\mathcal{N}$ (absolute), $T_r$, and $T_v$ for the expansion I is given in Table I, jointly with the vibrational contribution $C_{P,v}$ to the molar heat capacity at constant pressure. The data interpolated using Eq. (25) at steps of 0.05 mm are indicated in parenthesis.

The experimental density number of the four expansions is shown in Fig. 2 in the form $\ln(\mathcal{N}/\mathcal{N}_0)$, for $\mathcal{N}_0^{I}=81.2$, $\mathcal{N}_0^{II}=41.2$, $\mathcal{N}_0^{III}=17.6$, and $\mathcal{N}_0^{IV}=9.2$ mol/m$^3$, the nominal

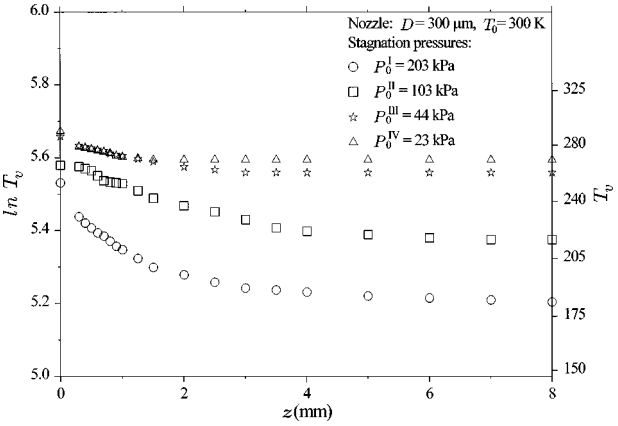


FIG. 4. Vibrational temperatures (smoothed) in supersonic expansions I–IV of $CO_2$.

TABLE I. Expansion I: Supersonic jet of $CO_2$ through a circular nozzle of diameter $D=300$ μm, generated at a nominal stagnation pressure $P_0^{I}=203$ kPa and temperature $T_0=300$ K. Absolute molar density number ($\mathcal{N}$), rotational temperature ($T_r$), vibrational temperature ($T_v$), and vibrational contribution to the heat capacity ($C_{P,v}$) at constant pressure. Interpolated values are given in parenthesis.

| $m$ or $l$ | $z_m$ mm | $\mathcal{N}$[a] mol/m$^{-3}$ | $T_r$[a] K | $T_v$[b] K | $C_{P,v}$[c] J K$^{-1}$ mol$^{-1}$ |
|---|---|---|---|---|---|
| 1 | 0.0 | 51.50 | 259.5 | 252.5 | 5.62 |
| 2 | 0.05 | (31.90) | (215.0) | (246) | 5.33 |
| 3 | 0.10 | (20.50) | (181.0) | (241) | 5.11 |
| 4 | 0.15 | (13.70) | (155.0) | (238) | 4.97 |
| 5 | 0.20 | (9.60) | (135.0) | (235) | 4.83 |
| 6 | 0.25 | (7.00) | (120.0) | (233) | 4.74 |
| 7 | 0.30 | 4.76 | 108.6 | 230 | 4.60 |
| 8 | 0.35 | 4.12 | 102.0 | 228 | 4.51 |
| 9 | 0.40 | 3.48 | 95.6 | 226 | 4.42 |
| 10 | 0.45 | 3.01 | 90.5 | 224 | 4.33 |
| 11 | 0.50 | 2.55 | 85.5 | 223 | 4.28 |
| 12 | 0.55 | 2.26 | 82.6 | 221 | 4.19 |
| 13 | 0.60 | 1.97 | 79.7 | 220 | 4.14 |
| 14 | 0.65 | 1.68 | 78.9 | 219 | 4.09 |
| 15 | 0.70 | 1.40 | 78.2 | 218 | 4.05 |
| 16 | 0.80 | 1.08 | 77.6 | 215 | 3.91 |
| 17 | 0.90 | 0.83 | 76.9 | 212 | 3.77 |
| 18 | 1.00 | 0.660 | 76.2 | 210 | 3.67 |
| 19 | 1.25 | 0.390 | 73.0 | 205 | 3.44 |
| 20 | 1.50 | 0.272 | 70.4 | 200 | 3.21 |
| 21 | 2.00 | 0.149 | 64.0 | 196 | 3.02 |
| 22 | 2.50 | 0.091 | 58.4 | 192 | 2.84 |
| 23 | 3.00 | 0.0607 | 54.9 | 189 | 2.71 |
| 24 | 3.50 | 0.0425 | 52.1 | 188 | 2.66 |
| 25 | 4.00 | 0.0320 | 48.6 | 187 | 2.62 |
| 26 | 5.00 | 0.0198 | 43.6 | 185 | 2.53 |
| 27 | 6.00 | 0.0128 | 40.2 | 184 | 2.48 |
| 28 | 7.00 | 0.0091 | 36.3 | 183 | 2.44 |
| 29 | 8.00 | 0.0068 | 34.1 | 182 | 2.40 |

[a]Experimental.
[b]Experimental (smoothed).
[c]From Eq. (9).

stagnation density numbers at the stagnation temperature $T_0=300$ K. Though the ratio $\ln(\mathcal{N}/\mathcal{N}_0)$ shown in Fig. 2 looks similar for the four expansions, a close scrutiny of the numerical values reveals a slight decrease at large distances $z$ for the expansions generated at higher stagnation pressures. By virtue of the mass conservation principle, which implies the invariance of the product $\mathcal{N}v\mathcal{A}$, with $\mathcal{A}$ the area of a stream tube, this decrease in density is likely related to the increase of flow velocity due to condensation, as discussed below.

The experimental rotational temperature and the experimental (smoothed) vibrational temperatures are shown in Figs. 3 and 4, respectively.

The procedure described in Sec. II to relate the energy $\chi$ released by condensation with the number density and the temperatures has been carried out assuming a functional dependence of the rotation–translation collision number on the translational temperature of the form[64]

$$Z_r = Z_r^{\infty}\left[1+\frac{\pi^{3/2}}{2}\left(\frac{b}{T_t}\right)^{1/2}+\left(\frac{\pi^2}{4}+\pi\right)\left(\frac{b}{T_t}\right)\right]^{-1}, \qquad (26)$$

with $Z_r^{\infty}=17.9$ and $b=100$ K, parameters which lead to a compromise between the experimental results[38] and the Monte Carlo predictions[65] for $CO_2$. It is worth noticing that for all four expansions investigated, the translational temperature derived from Eqs. (13) to (15) is encompassed between the rotational temperature and the isentropic temperature.

The energy $\chi$ released along expansions I–IV by condensation, and the energy $E_v$ released by vibrational cooling, are depicted in Figs. 5(a)–5(d) jointly with the rotational and translational temperatures. The isentropic temperature for $\gamma=1.4$ is included as a guide for the eye.

As shown in Fig. 5(a) for the expansion at higher stagnation pressure the onset of condensation, represented by the release of condensation energy $\chi$, occurs sharply at about two nozzle diameters, progressing markedly along the next eight nozzle diameters. Then it tends to stabilize and, at about 25 nozzle diameters, little energy is being released by condensation. Vibrational cooling also transfers energy to the flow. Along the first two nozzle diameters vibrational energy transfer appears to be dominant, but as the expansion progresses it tends to stabilize at about 1/5 of the condensation energy. Due to the relatively high density number in expansion I, the collisional rate is high enough to maintain the rotational and translational temperatures almost in equilibrium, at values substantially larger than those predicted by the isentropic approximation for $\gamma=1.4$

The results for expansions II and III, at lower stagnation pressures, are shown in Figs. 5(b) and 5(c). As can be noticed, less condensation energy and vibrational energy is released, and the lag between rotational and translational temperatures tends to increase along the expansion.

Finally, for expansion IV, at the lowest stagnation pressure that can be studied with the present experimental equipment, the condensation energy can hardly be detected. This is shown in Fig. 5(d), jointly with the rotational temperature and the translational temperature which, in this case, is close to the isentropic temperature of a perfect gas of $\gamma=1.4$.

According to Eq. (16) the condensation energy and the vibrational energy, partially converted into flow kynetic energy, tend to increse the flow velocity with respect to the isentropic velocity. The velocity increments $\Delta v$ of the four expansions are shown in Fig. 6.

In Fig. 7 the relaxation time derived here for expansion II ($P_0=103$ kPa and $T_0=300$ K) is compared with the theoretical relaxation times derived from a Monte Carlo simulation in a bulb, and from the thermal conduction model in a supersonic expansion.[65] In the range above 60 K the agreement with the thermal conduction model is satisfactory. On the contrary, at lower temperatures the theory predicts a too short relaxation time, a result which appears not to be compatible with the present experimental results. If the theoretical relaxation times for $T_t \leqslant 60$ K are replaced in Eq. (13), jointly with the experimental rotational temperatures, the resulting translational temperature becomes considerably lower than the isentropic temperature for a perfect gas of $\gamma=1.4$, a result somewhat difficult to justify.

As far as the onset of massive condensation at about two nozzle diameters, present results are consistent with those

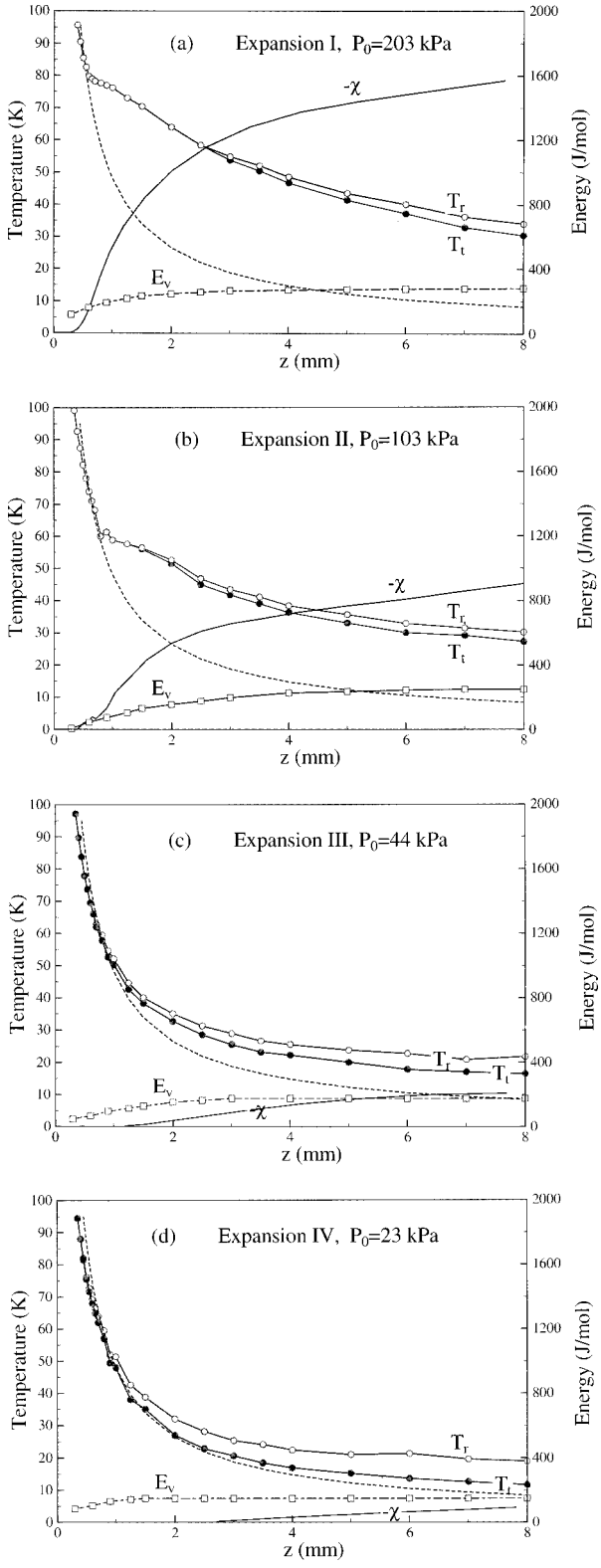


FIG. 5. Rotational temperature ($T_r$), translational temperature ($T_t$), condensation energy ($\chi$), and vibrational energy ($E_v$), in expansions I–IV of $CO_2$. Isentropic temperature (---) for $\gamma=1.4$ according to Ref. 60.

from Rayleigh scattering measurements in $CO_2$. However, no quantitative comparison is possible due to the qualitative nature of the Rayleigh scattering data reported.[17]

Monte Carlo simulation of the thermodynamic properties of $(CO_2)_n$ clusters of size up to $n=13$ show that, in general,

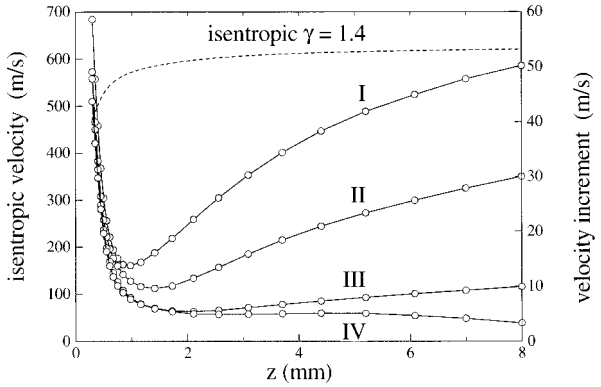


FIG. 6. Increments of flow velocity in expansions I–IV, with respect to the isentropic flow velocity (---) of $CO_2$.

such clusters are not stable at temperatures above 80 K.[66] This agrees too with the trends shown in Figs. 5(a) and 5(b), where the sudden change of slope of $T_r$ near this temperature may be related to the fast growth of the energy $\chi$ released by condensation.

Other experiments reporting condensation in supersonic expansions of $CO_2$ (Refs. 40 and 41) have been carried out under experimental conditions rather different from the present ones, this precluding any quantitative comparison.

The energy $\chi$ released by condensation, given in Fig. 5, may help estimate the molar fraction of condensed $CO_2$. As has been shown,[40,53] the dimer formation is predominant at the beginning of the expansion. In present experiments this can be conjectured to occur between one and two nozzle diameters, downstream in the expansion. On the basis of several intermolecular potentials reported for $CO_2$ (Refs. 67–71) the binding energy in the dimer amounts to about $U_b = -250\ \mathrm{cm}^{-1}$/monomer. This implies that a fraction of 10% of monomers involved in dimers should transfer to the jet an energy on the order of $\chi = -300$ J/mol. Comparing with Fig. 5(a), this leads us to conclude that in expansion I the fraction of monomers forming dimers should remain below 10% in the range between one and two nozzle diameters. At distances $z > 0.6$ mm, larger than two nozzle diameters, the condensation may be expected to evolve very fast, with sudden formation of larger clusters and/or microdroptets. Earlier attempts to identify small size $CO_2$ clusters in the first nozzle diameters of the expansion by means of CARS lead to ambiguous conclusions.[47,50,51] In a recent work, the influence of the stagnation pressure onto the formation rate of $CO_2$ dimer has been investigated, leading to the conclusion that up to 15% of the dimer was formed in the initial phase of an expansion of $CO_2$ through a slit nozzle of width 100 $\mu$m, under stagnation pressure of 400 kPa.[52,53]

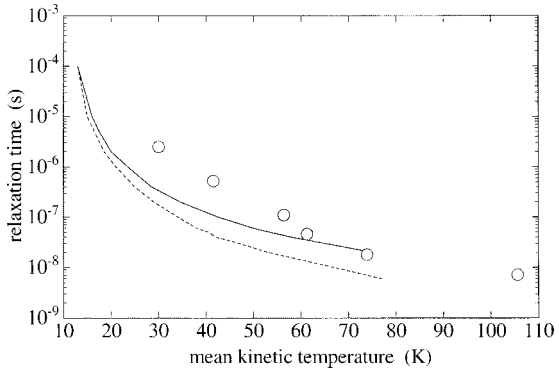


FIG. 7. Rotational relaxation time of $CO_2$ at $P_0 = 103$ kPa and $T_0 = 300$ K (---) Monte Carlo simulation in a bulb, (—) thermal conduction model in a supersonic expansion, according to Ref. 65.

Molecular dynamics calculations[72] predict a binding energy encompassed between $U_b = -1100$ and $U_b = -1650\ \mathrm{cm}^{-1}$/monomer for amorphous clusters larger than 20 monomers. An average value of $U_b = -1400\ \mathrm{cm}^{-1}$/monomer may tentatively be assumed in order to estimate the fraction of condensed monomers in present expansions. From the condensation energy $\chi$ at $z = 8$ mm (Fig. 5), the former assumption yields a fraction of 9% of condensed monomers in expansion I, 5% in expansion II, 1.5% in expansion III, and 0.5% in expansion IV. Of course, these figures are subject to large uncertainty. They, however, provide a first quantitative estimate of the condensation in a region of the flow field, relatively close to the nozzle, where other quantitative methods are hardly applicable.

A search for the crystalline phase of $CO_2$ in expansions I–IV has been carried out in the region of the strong $E_g$ librational mode[73,74] at 73.5 $\mathrm{cm}^{-1}$, and in the region of the upper component of the main Fermi diad,[75] at 1384.0 $\mathrm{cm}^{-1}$. No evidence of cystalline $CO_2$ has been found. On the contrary, amorphous or liquid $CO_2$ is neatly observed in expansion I at 1385.8 $\mathrm{cm}^{-1}$, in a proportion of about 4% at $z = 8$ mm. Additional contributions from the amorphous phase overlapped by the strong band of the monomer at 1388.2 $\mathrm{cm}^{-1}$ cannot be excluded due to the low spectral resolution, about 1 $\mathrm{cm}^{-1}$, of present experiment.

As shown in Fig. 5, the maximum lag between rotational and translational temperature amounts to about 4 K for expansions I and II, 6 K for expansion III, and 8 K for expansion IV. These lags appear to be smaller than reported before, probably due to the large rotational collision number $Z_r = 10$ considered in previous work.[17]

The vibrational energy released along the vibrational cooling has been mentioned to be related to condensation.[17,41] From Fig. 5 the liberation of vibrational energy appears to occur prior to the onset of condensation, particularly for expansion I, where the contribution of vibration energy is more pronounced. A more detailed study of this point is required, however.

A major consequence of condensation is the increase of flow velocity[39,76] with respect to the isentropic velocity for a perfect gas. This effect is noticeable in Fig. 6 for distances above 2 mm from the nozzle, with flow velocity increments of 50 m/s for expansion I, 30 m/s for expansion II, 10 m/s for expansion III, and 4 m/s for expansion IV, at a distance of 8 mm from the nozzle. These values are slightly smaller than the ones reported for $CO_2$ at large distance from the nozzle ($z/D = 1000$).[39,76] From Fig. 5 there is some evidence that for $z > 8$ mm the condensation process should still liberate some energy, with a slight increase in flow velocity at larger distances. Indeed, due to the limited pumping capacity of the

present expansion chamber, the relatively high residual pressure ($P_r \geqslant 0.4$ hPa) originates a normal shock front before the complete rotational relaxation has been reached. The residual pressure has been controlled in such a way that the Mach disk of expansions I–IV has been located at $z = 10$ mm from the nozzle. Data up to $z = 8$ mm appear to be free from shock front perturbations.

Finally, it should be mentioned that velocity increments for $z < 1$ mm, similar for all four expansions, are not due to condensation. They may be attributed to the non ideal form of present nozzle and to the curvature of the flow field lines in the first nozzle diameters.

## V. CONCLUSIONS

The present approach is aimed to the quantification of the relationships between the main macroscopic quantities in molecular supersonic jets on the basis of high sensitivity Raman spectroscopy data. The results shown here should be considered just demostrative of the current possibilities of Raman spectroscopy for jet diagnostics. No doubt, the scope of present experimental data can be improved substantially by augmenting the performance of the expansion chamber, in order to cover a wider range of stagnation pressures, stagnation temperatures, and residual pressures. The accuracy of the experimental data can also be improved with aid of a more powerful laser exciting source than the one used here, and/or by means of spectral average over longer data acquisition periods.

Further instrumental improvements are still possible with moderate effort. The optical collection system of the Raman signal can be adapted to the acquisition of experimental data within the first nozzle diameter of the expansion, this allowing for a more accurate description of the boundary conditions of the jet at the onset of the supersonic regime. Inclusion of Rayleigh scattering data, in principle possible with minor modifications of the present equippment, should provide information about the size distribution of aggregates.

As far as the information derived from the $CO_2$ supersonic jets investigated here, present results widen and confirm, within a quantitative frame, the qualitative conclusions from previous works. This shows to what extent linear Raman spectroscopy is a mature diagnostics tool for molecular hypersonics at laboratory scale, based on relatively simple instrumentation at moderate cost.

## ACKNOWLEDGMENTS

We are indebted to V. Herrero for many valuable discussions, and to R. Escribano, J. M. Fernández, and J. Ortigoso for the revision of the manuscript. The Spanish Dirección General de Investigación Científica y Técnica, DGICYT, is acknowledged for financial support (Research Project No. PB94-1526).

## APPENDIX

The points, of coordinates $(0,0,z_m)$, the experimental quantities $\mathcal{N}$, $T_r$, $T_v$, $C_{P,v}$, and the associated quantities $A$, $B$, and $C$, defined below, may be described by the discrete variables $m = 1,2,3,...$, and $l \leqslant m$. The translational temperature at the point $m$ becomes then

$$T_t(m) = \left(\frac{\mathcal{N}(m)}{\mathcal{N}^*}\right)^{2/3}\left[T^* + \frac{1}{2}\sum_{l=1}^{m} A(l) + B(l) + C(l)\right], \tag{A1}$$

with $A(1) = B(1) = C(1) = 0$ by virtue of the boundary conditions; $A(l)$, $B(l)$, and $C(l)$ are defined, for $l > 1$, as

$$A(l) = -\frac{N_r}{3}\left(\frac{\mathcal{N}(m)}{\mathcal{N}^*}\right)^{-2/3}[T_r(l+1) - T_r(l-1)], \tag{A2}$$

$$B(l) = -\frac{2}{3R}\left(\frac{\mathcal{N}(m)}{\mathcal{N}^*}\right)^{-2/3} C_{P,v}(l)[T_v(l+1) - T_v(l-1)], \tag{A3}$$

and

$$C(l) = -\frac{2}{3R}\left(\frac{\mathcal{N}(m)}{\mathcal{N}^*}\right)^{-2/3}[\chi(l+1) - \chi(l-1)], \tag{A4}$$

It should be noted that the first point considered in the expansion is $m = 1$, corresponding to $z = 0$. For the consistency of Eqs. (A1)–(A4) with the boundary conditions this implies the identities $\mathcal{N}^* = \mathcal{N}(1)$ and $T^* = T_t(1)$.

[1] M. J. Zucrow and J. D. Hoffman, *Gas Dynamics* (Wiley, New York, 1976), Vol. I.
[2] J. D. Anderson, Jr., *Modern Compressible Flow* (McGraw–Hill, New York, 1990).
[3] K. A. Bütefisch and D. Vennemann, Prog. Aerosp. Sci. **15**, 217 (1974).
[4] F. Robben and L. Talbot, Phys. Fluids **9**, 653 (1966).
[5] P. V. Marrone, Phys. Fluids **10**, 521 (1967).
[6] H. C. W. Beijering and N. F. Verster, Physica C **111**, 327 (1981).
[7] T. Holz and E. P. Munz, Phys. Fluids **26**, 2425 (1983).
[8] J. D. Lambert, *Vibrational and Rotational Relaxation in Gases* (Clarendon, Oxford, 1977).
[9] B. W. Schumacher and E. O. Gadamer, Can. J. Phys. **36**, 659 (1958).
[10] E. P. Muntz, Phys. Fluids **5**, 80 (1962).
[11] J. W. L. Lewis, *Proceedings of the 16th International Symposium on Rarefied Gas Dynamics*, Progress in Astronautics and Aeronautics Vol. 117 (AIAA, Washington, DC, 1989), p. 107.
[12] A. E. Belikov and R. G. Sharafutdinov, Chem. Phys. Lett. **241**, 209 (1995).
[13] D. H. Levy, Annu. Rev. Phys. Chem. **31**, 197 (1980).
[14] R. Jost, in *Low Temperature Molecular Spectroscopy*, edited by R. Fausto, NATO ASI Series C Vol. 483 (Kluwer, Dordrecht, 1996), p. 249.
[15] I. F. Silvera and F. Tommasini, Phys. Rev. Lett. **37**, 136 (1976).
[16] G. Luijks, S. Stolte, and J. Reuss, Chem. Phys. **62**, 217 (1981).
[17] R. G. Shabram, A. E. Beylich, and E. M. Kudriavtsev, in Ref. 11, p. 168.
[18] G. Tejeda, B. Maté, J. M. Fernández-Sánchez, and S. Montero, Phys. Rev. Lett. **76**, 34 (1996).
[19] J. W. Nibler, Annu. Rev. Phys. Chem. **38**, 349 (1987).
[20] M. Lefebvre, B. Chanetz, T. Pot, P. Bouchardy, and Ph. Varghese, La Recherche Aerosp. **4**, 295 (1994).
[21] M. Lefebvre, M. Pealat, and J. Strempel, Opt. Lett. **17**, 1806 (1992).
[22] M. Pealat and M. Lefebvre, Appl. Phys. B: Photophys. Laser Chem. **53**, 23 (1991).
[23] H. Wong and J. R. Ferron, *Proceedings of the 18th International Symposium on Rarefied Gas Dynamics*, Progress in Astronautics and Aeronautics Vol. 158 (AIAA, Washington, DC, 1993), p. 27.
[24] O. Faucher, F. Aguillon, and R. Campargue, J. Chem. Phys. **94**, 4141 (1991).
[25] F. Aguillon, A. Lebéhot, J. Rousseau, and R. Campargue, J. Chem. Phys. **86**, 5246 (1987).
[26] W. D. Williams and I. W. L. Lewis, AIAA J. **13**, 709 (1975).
[27] J. J. Barrett and A. B. Harvey, J. Opt. Soc. Am. **65**, 392 (1975).
[28] D. R. Miller and R. P. Andres, J. Chem. Phys. **46**, 3418 (1967).

[29] R. J. Gallagher and J. B. Fenn, J. Chem. Phys. **60**, 3487 (1974).
[30] S. Yamazaki, M. Taki, and Y. Fujitani, J. Chem. Phys. **74**, 4476 (1981).
[31] L. Abad, D. Bermejo, V. J. Herrero, J. Santos, and I. Tanarro, J. Phys. Chem. (submitted).
[32] A. E. Beylich, AIAA J. **8**, 965 (1970).
[33] A. E. Beylich, Phys. Fluids **14**, 898 (1971).
[34] O. F. Hagena and W. Obert, J. Chem. Phys. **56**, 1793 (1972).
[35] W. G. Dorfeld and J. B. Hudson, J. Chem. Phys. **59**, 1253 (1973).
[36] W. G. Dorfeld and J. B. Hudson, J. Chem. Phys. **59**, 1261 (1973).
[37] P. J. Wantuck, R. H. Krauss, and J. E. Scott, Jr., in Ref. 11, p. 336.
[38] S. Yamazaki, M. Taki, and Y. Fujitani, *Proceedings of the 12th International Symposium on Rarefied Gas Dynamics*, Progress in Astronautics and Aeronautics Vol. 74. Part II (AIAA, New York, 1981), p. 802.
[39] N. G. Zharkova, V. V. Prokoev, A. K. Rebrov, P. A. Skovorodko, and V. N. Yarygin, *Proceedings of the 11th International Symposium on Rarefied Gas Dynamics* (CEA, Paris, 1979), Vol. 11, p. 1141.
[40] Yu. S. Kusner, A. K. Rebrov, B. E. Semyachkin, and A. A. Vostrikov, in Ref. 39, p. 1119.
[41] V. N. Yarygin, P. A. Skovorodko, N. G. Gorchakova, G. A. Khramov, and O. A. Nerushev, *Proceedings of the 14th International Symposium on Rarefied Gas Dynamics* (University of Tokyo Press, Tokyo, 1984), Vol. II, p. 95.
[42] M. A. Walsh, T. H. England, T. R. Dyke, and B. J. Howard, Chem. Phys. Lett. **142**, 265 (1987).
[43] K. W. Jucks, Z. S. Huang, R. E. Miller, G. T. Fraser, A. S. Pine, and W. J. Lafferty, J. Chem. Phys. **88**, 2185 (1988).
[44] G. T. Fraser, A. S. Pine, W. J. Lafferty, and R. E. Miller, J. Chem. Phys. **87**, 1502 (1987).
[45] M. J. Weida, J. M. Sperhac, and D. J. Nesbitt, J. Chem. Phys. **103**, 7685 (1995).
[46] J. A. Barnes and T. E. Gough, J. Chem. Phys. **86**, 6012 (1987).
[47] G. A. Pubanz, M. Maroncelli, and J. W. Nibler, Chem. Phys. Lett. **120**, 313 (1985).
[48] J. W. Nibler and G. A. Pubanz, in *Advances in Non-linear Spectroscopy*, edited by R. J. H. Clark and R. Hester (Wiley, New York, 1988).
[49] H. D. Barth and F. Huisken, Chem. Phys. Lett. **169**, 198 (1990).
[50] H. D. Barth and F. H. Huisken, in *Coherent Raman Spectroscopy*, edited by G. Marowsky and V. V. Smirnov, Springer Proceedings in Physics Vol. 63 (Springer, Berlin, 1992), p. 242.
[51] K. W. Brown, A. D. Richardson, N. H. Rich, and J. W. Nibler, in *Proceedings of the 13th International Conference on Raman Spectroscopy*, 1992, p. 204.
[52] F. Huisken, L. Ramonat, V. V. Smirnov, O. M. Stelmakh, and A. A. Vigasin, Proc. SPIE **2205**, 95 (1995).
[53] F. Huisken, L. Ramonat, J. Santos, V. V. Smirnov, O. M. Stelmakh, and A. A. Vigasin, J. Mol. Struct. **410**, 47 (1997).
[54] L. K. Randeniya and M. A. Smith, J. Chem. Phys. **93**, 661 (1990).
[55] G. Herzberg, *Molecular Spectra and Molecular Structure* (Krieger, Malabar, 1991), Vol. II, Chapter V.
[56] R. A. Alberty, *Physical Chemistry*, 7th ed. (Wiley, New York, 1987).
[57] The characteristic rotational temperature of $CO_2$ is $\Theta_r = 0.56$ K.
[58] C. G. M. Quah, J. B. Fenn, and D. R. Miller, in Ref. 39, p. 885.
[59] H. Ashkenas and F. S. Sherman, *Proceedings of the 4th International Symposium on Rarefied Gas Dynamics*, 1964 (unpublished), Sec. 7, Vol. 2, p. 84.
[60] D. R. Miller, in *Atomic and Molecular Beam Methods*, edited by G. Scoles (Oxford University Press, New York, 1988), Vol. I.
[61] G. Tejeda, J. M. Fernández-Sánchez, and S. Montero, Appl. Spectrosc. **51**, 265 (1997).
[62] R. Campargue, J. Phys. Chem. **88**, 4466 (1984).
[63] G. Tejeda, B. Maté, and S. Montero, J. Chem. Phys. **103**, 568 (1995).
[64] J. G. Parker, Phys. Fluids **2**, 449 (1959).
[65] B. R. Cameron and P. W. Harland, J. Chem. Soc. Faraday Trans. **89**, 3517 (1993).
[66] R. D. Etters, K. Flurchick, R. P. Pan, and V. Chandrasekharan, J. Chem. Phys. **75**, 929 (1981).
[67] A. I. Kitaigorodskii, K. V. Mirskaya, and V. V. Nauchitel, Sov. Phys. Crystallogr. **14**, 769 (1970).
[68] C. S. Murthy, K. Singer, and I. R. Mc Donald, Mol. Phys. **44**, 135 (1981).
[69] C. S. Murthy, S. F. O'Shea, and I. R. Mc Donald, Mol. Phys. **50**, 531 (1983).
[70] P. Procacci, R. Righini, and S. Califano, Chem. Phys. **116**, 171 (1987).
[71] S. L. Mayo, B. D. Olafson, and W. Goddard III, J. Phys. Chem. **94**, 8897 (1990).
[72] G. Cardini, V. Schettino, and M. L. Klein, J. Chem. Phys. **90**, 4441 (1989).
[73] J. E. Cahill and G. E. Leroi, J. Chem. Phys. **51**, 1324 (1969).
[74] A. Anderson and T. S. Sun, Chem. Phys. Lett. **8**, 537 (1971).
[75] R. Ouillon, P. R. Ranson, and S. Califano, J. Chem. Phys. **83**, 2162 (1985).
[76] A. B. Bailey, P. Dawbarn, and M. R. Busby, AIAA J. **14**, 91 (1976).